

Analysis of a Radial Flux Air-Cored Permanent Magnet Machine with a Double-sided Rotor and Non-overlapping Windings

PhD – Oral Examination

Peter Jan Randewijk

**Stellenbosch University, Faculty of Engineering,
Dep. of Electrical & Electronic Engineering,
Electrical Machines Research Group**

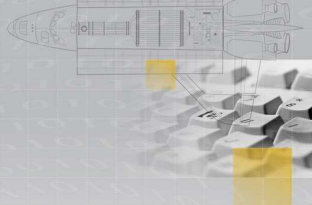
<http://research.ee.sun.ac.za/emr/>

Supervisor – Prof. M.J. Kamper

17 February 2012

Outline

- 1 Introduction
- 2 Subdomain analysis method
- 3 Winding Configuration
- 4 Back-EMF Calculation
- 5 Torque Calculation
- 6 Conclusion
- 7 Bibliography

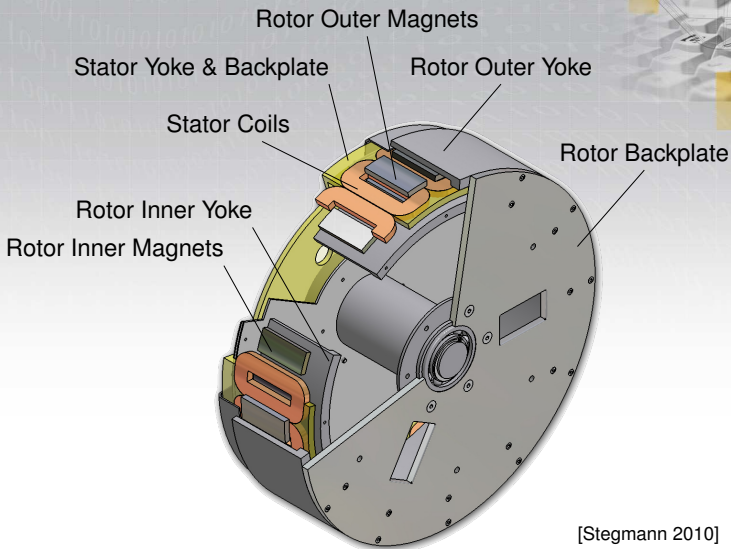


Introduction

- The Radial Flux Air-cored Permanent Magnet (RFAPM) machine is a new type of machine
- The RFAPM machine is a dual of the Axial Flux Air-cored Permanent Magnet (AFAPM) machine with a double-sided rotor and double layer, non-overlapping, air-cored windings, [Kamper et al, 2008]
- The RFAPM machine was first presented by [Randewijk et al, 2007]
- The salient features of the RFAPM machine:
 - cylindrically shaped double-sided rotor
 - air-cored stator
 - non-overlapping windings

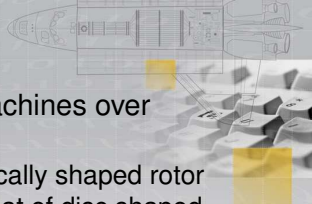


Introduction (*cont.*)



[Stegmann 2010]

Introduction (*cont.*)



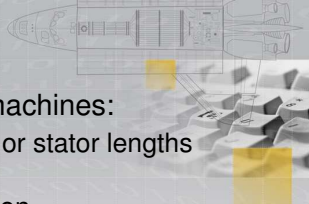
- The advantages of RFAPM machines over AFAPM machines:
 - structural integrity of cylindrically shaped rotor yokes is much higher than that of disc shaped rotor yokes
 - ☞ [Stegmann & Kamper, 2009] – more than 30 % lower mass for a similar 6.75 kW machine
- The advantages of an air-cored machine:
 - no stator iron losses
 - ☞ higher efficiency
 - no cogging torque
 - ☞ lower wind cut-in speeds
- The advantages of non-overlapping windings:
 - lower end-winding length
 - lower copper losses
 - ☞ higher efficiency
 - ☞ higher torque per copper volume ratio



Introduction (*cont.*)

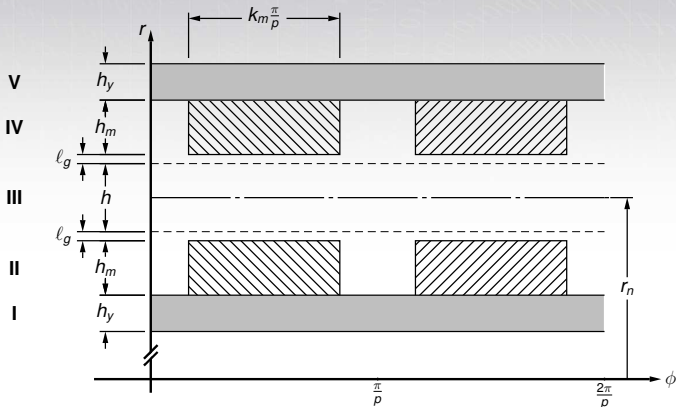
- Application fields for RFAPM machines:
 - large diameter, short “stack” or stator lengths
 - multiple pole machines
 - ideal for direct drive application
 - ☞ small to medium direct drive, wind turbine generators

- Focus of Dissertation:
 - thorough analytical analysis of the RFAPM machine
 - reduce blind reliance on FEM
 - simplify calculation of back-EMF & torque
 - solve the ripple torque riddle



Subdomain analysis method

In order to analytically find the solution to the magnetic field inside the machine, the machine is divided into different 2D regions or subdomains



Subdomain analysis method (cont.)

- ➡ The RFAPM of [Stegmann & Kamper, 2011] where used as a Test Case.

Description	Symbol	Value
Number of pole-pairs	p	16
Number of coils per phase	q	8
Nominal stator radius	r_n	232 mm
Active stator/copper length	l	76 mm
Stator coil thickness/height	h	10 mm
N48 NdFeB PM thickness/height	h_m	8,2 mm
Rotor yoke thickness/height	h_y	8 mm
Air-gap length	l_g	1,0 mm

- The governing equations for the different regions or subdomain:

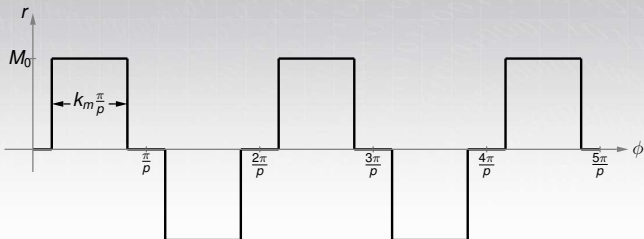
Regions	μ_r	Governing equation
I	$\mu_{r y}$	$\nabla^2 \vec{\mathbf{A}} = 0$
II	1	$\nabla^2 \vec{\mathbf{A}} = -\mu_0 (\nabla \times \vec{\mathbf{M}}_0)$
III	1	$\nabla^2 \vec{\mathbf{A}} = 0$
IV	1	$\nabla^2 \vec{\mathbf{A}} = -\mu_0 (\nabla \times \vec{\mathbf{M}}_0)$
V	$\mu_{r y}$	$\nabla^2 \vec{\mathbf{A}} = 0$

- Assumptions:

- in the rotor yokes, $\mu_{r|y}$ is *finite*
- in the rotor yokes, $\mu_{r|y}$ is *constant*
- the NdFeB grade N48 magnets, $\mu_{r, recoil|PM} \approx 1$

Subdomain analysis method (cont.)

- With the annulus shaped subdomains
- and a periodic forcing function of the radially magnetised PMs



where

$$\vec{M}_0 = \frac{\vec{B}_{rem}}{\mu_0}$$

- the solution to the partial differential equations has a known Fourier series expansion form.

Subdomain analysis method (cont.)

☞ General solution:

$$A_{z,gen}(r, \phi) = \sum_{m=1,3,5,\dots}^{\infty} (C_m r^{mp} + D_m r^{-mp}) \cos mp\phi$$

☞ Particular solution:

$$A_{z,part}(r, \phi) = \sum_{m=1,3,5,\dots}^{\infty} G_m \cos mp\phi$$

with

$$G_m = -\frac{4r_{cm}B_{rem} \cos mp\beta}{m^2 p \pi}$$

and

$$\beta = \left(\frac{1 - k_m}{2} \right) \frac{\pi}{p}$$

Subdomain analysis method (cont.)

- The relationship between the magnetic vector potential, the flux-density and the magnetic field intensity, is given by

$$\vec{\mathbf{B}} = \nabla \times \vec{\mathbf{A}} \quad \text{and}$$

$$\vec{\mathbf{H}} = \frac{\vec{\mathbf{B}}}{\mu}$$

- Using the boundary condition,

$$A_z^{(v)} = 0$$

on the inner – and outer boundary, and

Subdomain analysis method (cont.)

$$B_r^{(v)} = B_r^{(v+1)} \text{ and}$$

$$H_\phi^{(v)} = H_\phi^{(v+1)}$$

on the boundaries between two subdomains

- The solution for $C_m^{(v)}$ & $D_m^{(v)}$ for each subdomain, can be obtained from the following boundary matrix,

$$\begin{bmatrix}
 r_i^{mp} & r_i^{-mp} & \dots \\
 r_{ii}^{mp} & r_{ii}^{-mp} & -r_{ii}^{mp} & \dots \\
 r_{ii}^{mp-1} & -r_{ii}^{-mp-1} & -r_{ii}^{mp-1} & \dots \\
 & & r_{ii}^{mp} & \dots \\
 & & r_{iii}^{mp-1} & \dots \\
 & & r_{iii}^{mp-1} & \dots \\
 \vdots & \vdots & \vdots & \ddots
 \end{bmatrix} \cdot \begin{bmatrix} C_m^I \\ D_m^I \\ C_m^{II} \\ D_m^{II} \\ C_m^{III} \\ \vdots \end{bmatrix} = \begin{bmatrix} 0 \\ G_m^{II} \\ 0 \\ -G_m^{II} \\ 0 \\ \vdots \end{bmatrix}$$

Subdomain analysis method (cont.)

- with,

$$r_i = r_n - \frac{h}{2} - \ell_g - h_m - h_y$$

$$r_{ii} = r_n - \frac{h}{2} - \ell_g - h_m$$

$$r_{iii} = r_n - \frac{h}{2} - \ell_g$$

$$r_{iv} = r_n + \frac{h}{2} + \ell_g$$

$$r_v = r_n + \frac{h}{2} + \ell_g + h_m$$

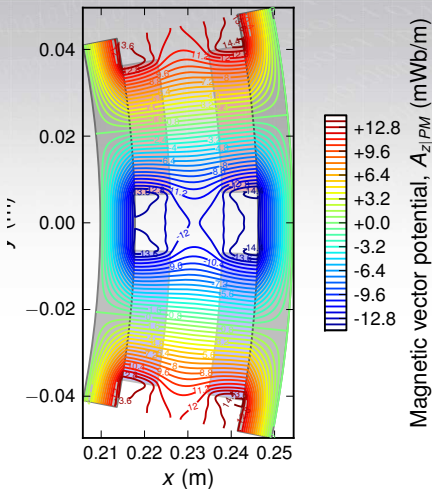
$$r_{vi} = r_n + \frac{h}{2} + \ell_g + h_m + h_y$$

the radii of the boundaries of the different subdomains

- $C_m^{(v)}$ & $D_m^{(v)}$ are only solved for,
 $m = 1, 3, 5, \dots, 27$
- This results in 140 values, completely describing the magnetic fields inside the RFAPM machine

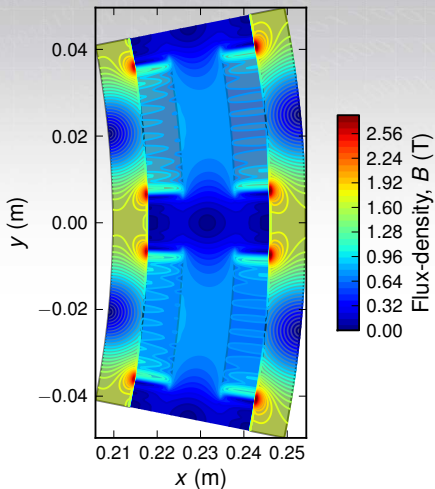
Subdomain analysis method (cont.)

- The magnetic vector potential, A_z , inside the RFAPM machine



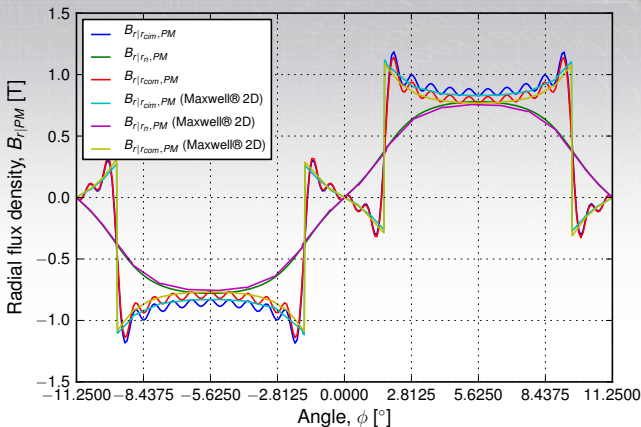
Subdomain analysis method (cont.)

- And from $\vec{\mathbf{B}} = \nabla \times \vec{\mathbf{A}}$, the magnitude of magnetic flux-density inside the RFAPM machine



Subdomain analysis method (cont.)

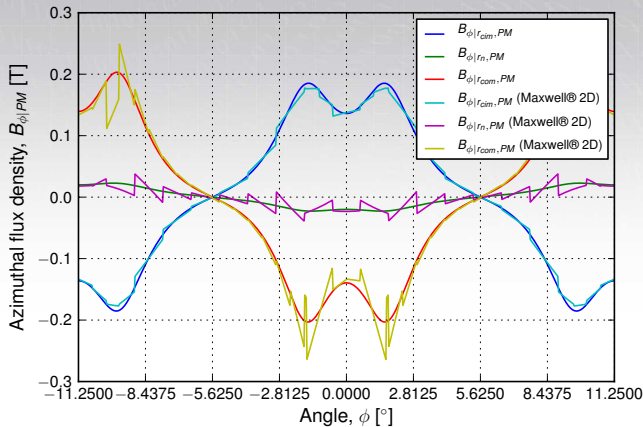
- The radial flux-density distribution in the centre of the PM – & stator regions



- ☞ The analytical solution is only calculated up to the 27th harmonic

Subdomain analysis method (cont.)

- The azimuthal flux-density distribution in the centre of the PM – & stator regions



Subdomain analysis method (cont.)

- We are however only interested in the magnetic vector potential & the radial flux-density in the stator region, i.e. region III, where

$$A_z^{III}(r, \phi) = \sum_{m=1,3,5,\dots}^{\infty} (C_m^{III} r^{mp} + D_m^{III} r^{-mp}) \cos mp\phi$$

and

$$B_r^{III}(r, \phi) = -\frac{1}{r} \cdot \sum_{m=1,3,5,\dots}^{\infty} mp(C_m^{III} r^{mp} + D_m^{III} r^{-mp}) \sin mp\phi$$

with C_m^{III} and D_m^{III} the coefficients obtained from the boundary conditions matrix

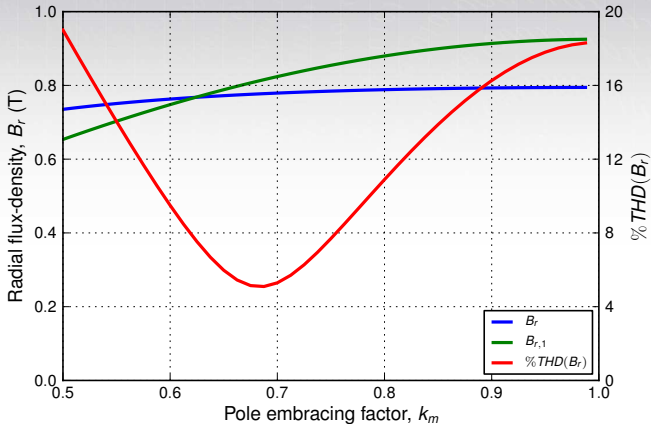
Subdomain analysis method (cont.)

- The magnetic vector potential allows us to calculate:
 - the flux-linkage from the stator's winding distribution
 - and hence the back-EMF induced
- The radial flux-density allows us to calculate:
 - the developed torque from the stator's current density distribution
- To try and simplify the calculation of the back-EMF & torque further
- and due to the fast solution provided by the analytical solution, 6 s vs. 300 s for the FEM solution,
- we varied the pole arc-width of the PMs to see if we could obtain a near sinusoidal radial flux-density distribution in the centre of the airgap



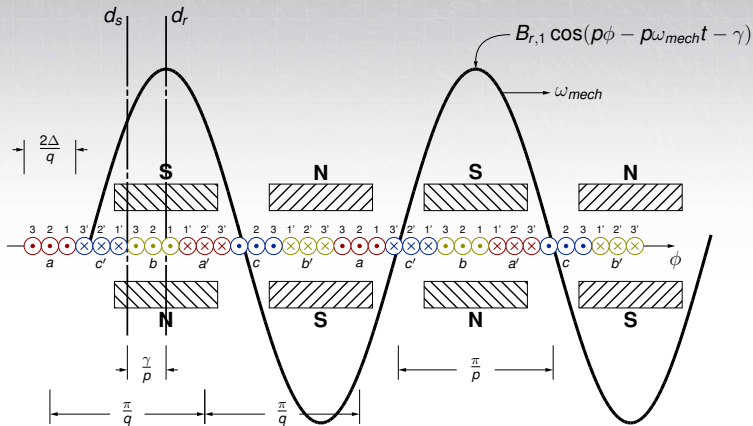
Subdomain analysis method (cont.)

- The peak, fundamental and %THD of the radial flux-density distribution as a function of k_m , in the centre of the stator winding:



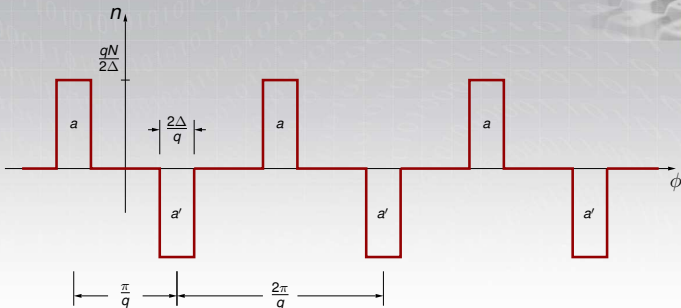
Winding Configuration

- The classical overlapping winding configuration with the number of coils, q , equal to the number of pole pairs, p



Winding Configuration (cont.)

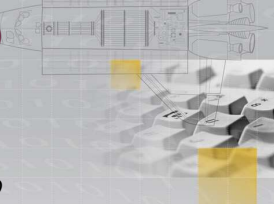
- The winding distribution for phase a ,



and can be given by the follow Fourier series,

$$n_{a|O}(\phi) = \sum_{n=1}^{\infty} b_{n|n,O} \sin(nq\phi)$$

Winding Configuration (cont.)



with

$$b_{n|n,O} = -\frac{2qN}{\pi} \cdot k_{w,n|O}$$

where $k_{w,n}$, the *winding factor*, is defined as

$$k_{w,n|O} = k_{w,pitch,n|O} \cdot k_{w,slot,n|O}$$

with the pitch factor

$$k_{w,pitch,n|O} = 1,0$$

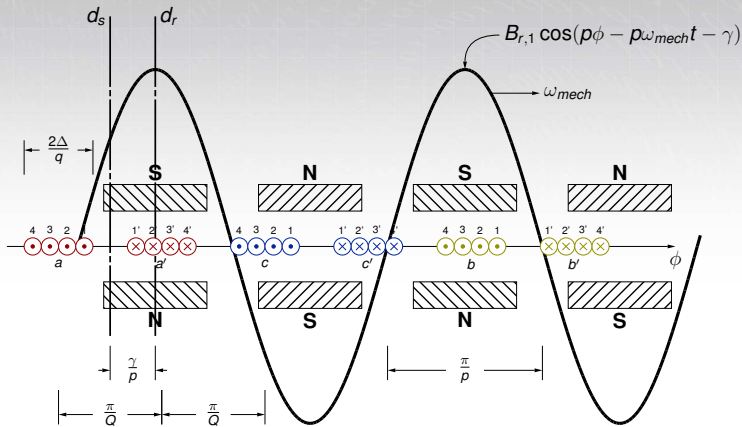
and the “virtual” slot – or coil-side width factor,

$$k_{w,slot,n|O} = \frac{\sin(n\Delta)}{n\Delta}$$

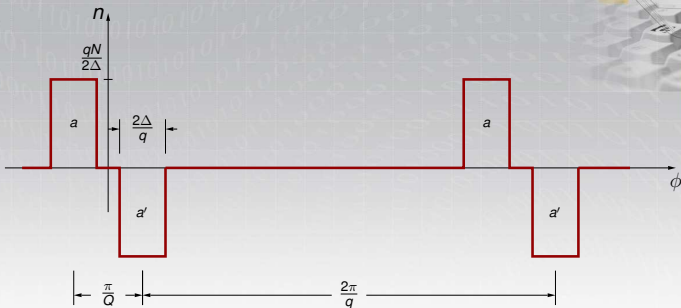


Winding Configuration (cont.)

- Uses single layer non-overlapping windings with the number of coils, q , half the number of pole paires, p



Winding Configuration (cont.)

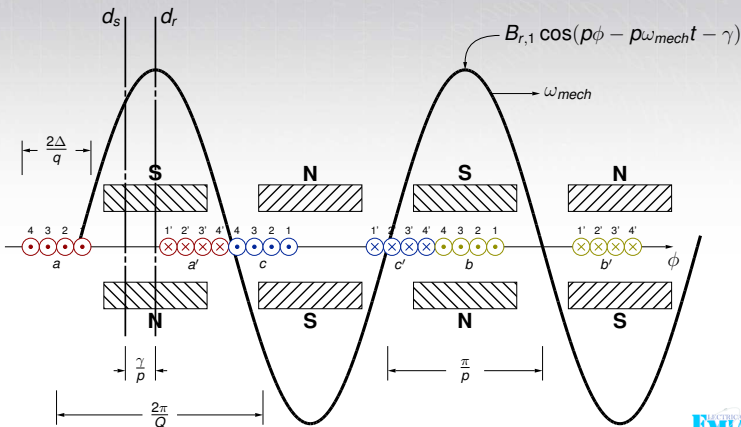


- Surprisingly, the only difference in die winding distribution for the single layer non-overlapping windings, is in the pitch factor

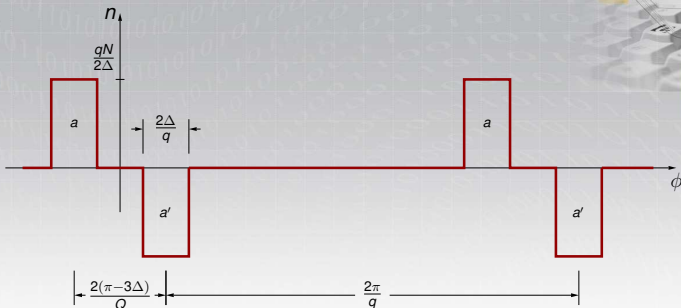
$$k_{w,pitch,n|l} = \sin\left(n\frac{\pi}{6}\right)$$

Winding Configuration (cont.)

- Uses double layer non-overlapping windings to maximise the flux-linkage per coil, but with the same number of coils. . .



Winding Configuration (cont.)



- Again the only difference in die winding distribution for the double layer non-overlapping windings, is in the pitch factor

$$k_{w,pitch,n||} = \sin\left(n\left(\frac{\pi}{3} - \Delta\right)\right)$$

Back-EMF Calculation



- Using Stokes' integral theorem and the winding distribution function,
- the amplitude of the flux-linkage in the stator windings, for the overlapping winding configuration, can be calculated as follows,

$$\Lambda_{a,b,c|O} = -\frac{1}{h} \int_{r_n - \frac{h}{2}}^{r_n + \frac{h}{2}} \frac{2qlN}{a} \sum_{m=1}^{\infty} k_{w,m|O} a_{m|A_z}^{III} dr$$

with

$$a_{m|A_z}^{III} = C_m^{III} r^{mp} + D_m^{III} r^{-mp}$$

Back-EMF Calculation (*cont.*)

- Assuming that the average flux-linkage is the same as that occurring at $r=r_n$ and
- Using only the fundamental component, i.e. $m=1$, the amplitude of the flux-linkage can be approximated as,

$$\Lambda_{a,b,c|O} \approx \frac{2qr_n l N}{ap} k_{w,1|O} B_{r,1}$$

- This will result in the amplitude for the back-EMF,

$$E_{a,b,c|O} \approx -\frac{2qr_n l N}{a} k_{w,1|O} B_{r,1} \omega_{mech}$$

- For the single – & double layer, non-overlapping windings,

Back-EMF Calculation (*cont.*)

- due to the fact that number of coils, q is half the number of pole pairs, p ,
- only the 2nd order space harmonics of the winding distribution, “ $n = 2m$ ”, will rotate at the same speed as the space harmonics of the magnetic vector potential (and that of the flux-density)
- Only considering “ $m = 1$ ” for the flux-density distribution,
- it implies we also only need to consider “ $n = 2$ ” for the winding distribution,
- so that for the non-overlapping winding configurations:

Back-EMF Calculation (cont.)

$$\Lambda_{a,b,c|I,II} \approx \frac{2qr_n l N}{ap} k_w{}_{,2|I,II} B_{r,1}$$

and

$$E_{a,b,c|I,II} \approx -\frac{2qr_n l N}{a} k_w{}_{,2|I,II} B_{r,1} \omega_{mech}$$

- This allows us to define a voltage constant, k_E
- similar to a “traditiona” brushless DC machine

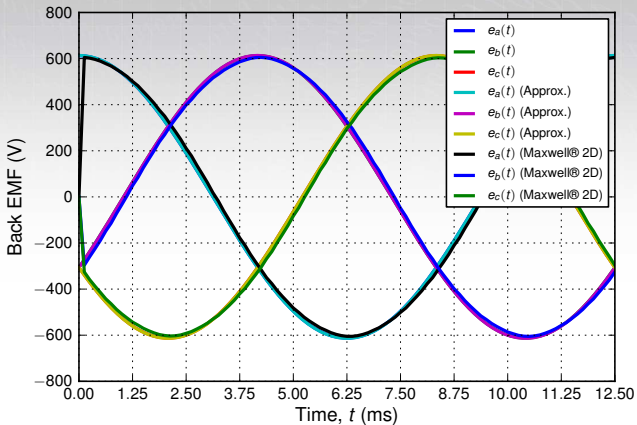
$$\hat{E}_f = k_E \omega_{mech}$$

with

$$k_E = \frac{2qr_n l N}{a} k_w \hat{B}_{r,1}$$

Back-EMF Calculation (cont.)

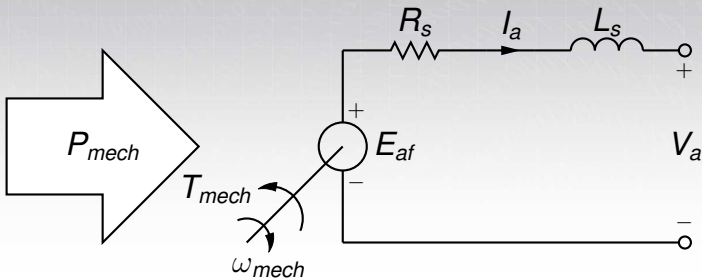
- The back-EMF comparison for the double layer, non-overlapping winding configuration



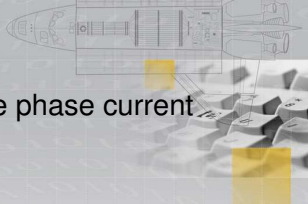
Torque Calculation

Average Torque

- From the equivalent circuit diagram of the RFAPM machine,



Torque Calculation (*cont.*)



- and with the back-EMF and the phase current regulated to be in phase,

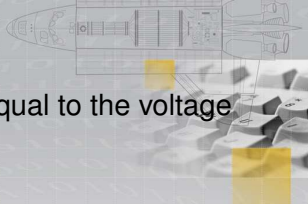
$$\begin{aligned}
 T_{mech} &= \frac{3E_{af}I_a}{\omega_{mech}} \\
 &= \frac{3\hat{E}_{af}\hat{I}_a}{2\omega_{mech}}
 \end{aligned}$$

where \hat{E}_{af} and \hat{I}_a are the peak values of the back-EMF and phase current respectively,

- the steady state torque developed by the machine can be written as

$$T_{mech} = k_T \hat{I}_s$$

Torque Calculation (*cont.*)



with the torque constant, k_T , equal to the voltage constant,

$$k_T = k_E = \frac{2qr_n\ell N}{a} k_w \hat{B}_{r,1}$$

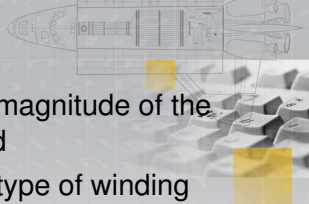
and the stator current space vector

$$\hat{l}_s = \frac{3}{2} \hat{l}_a$$

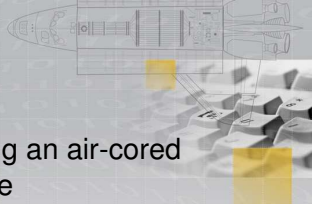
- Thus with the stator current space vector current regulated to be in-phase with the back-EMF space vector,

Torque Calculation (*cont.*)

- the torque will be equal to the magnitude of the stator current space vector and
- the RFAPM, regardless of the type of winding configuration used,
- looks like a “normal” brushless DC machine



Torque Calculation (*cont.*)



Ripple Torque

- With the RFAPM machine being an air-cored machine, i.e. no cogging torque
- The Lorentz method provides a quick and easy way in which the torque can be calculated
- From Lorentz's law, the volumetric force density can be calculated as

$$\begin{aligned}
 \vec{f}_v &= \vec{J} \times \vec{B} \\
 &= -J_z(\phi) B_\phi'''(r, \phi) \vec{a}_r + J_z(\phi) B_r'''(r, \phi) \vec{a}_\phi \\
 &= f_r \vec{a}_r + f_\phi \vec{a}_\phi
 \end{aligned}$$

- Only the azimuthal component of the volumetric force density, f_ϕ will contribute to “useful” torque

Torque Calculation (*cont.*)



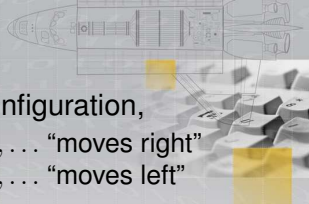
- From the winding distribution, assuming balanced sinusoidal currents,
- the three-phase current density distribution, for the overlapping winding configuration,

$$J_{z|O}(\phi) = \begin{cases} -\frac{3qI_p N}{ar_n h \pi} \sum_{n=1}^{\infty} k_{w,n|O} \sin(nq\phi + \omega t), & n = 3k-2 \\ -\frac{3qI_p N}{ar_n h \pi} \sum_{n=2}^{\infty} k_{w,n|O} \sin(nq\phi - \omega t), & n = 3k-1 \end{cases}$$

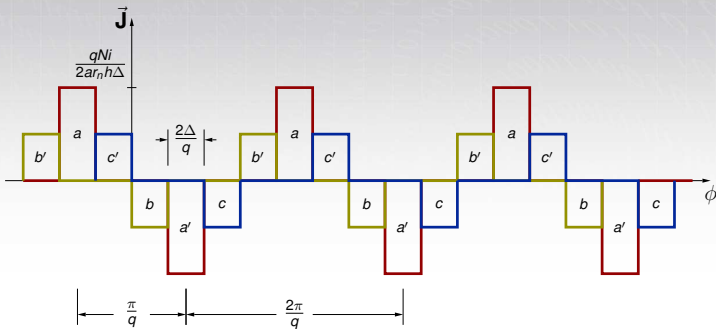
with $k \in \mathbb{N}_1$



Torque Calculation (*cont.*)



- For the overlapping winding configuration,
 - The $3k-2$ harmonics, 1, 4, 7, ... “moves right”
 - The $3k-1$ harmonics, 2, 5, 8, ... “moves left”



Torque Calculation (cont.)



- The three-phase current density distribution, for both the non-overlapping winding configuration, will be almost similar

$$J_{z|I,II}(\phi) = \begin{cases} -\frac{3qI_p N}{ar_n h \pi} \sum_{n=1}^{\infty} k_{w,n|I,II} \sin(nq\phi + \omega t), & n = 3k-1 \\ -\frac{3qI_p N}{ar_n h \pi} \sum_{n=2}^{\infty} k_{w,n|I,II} \sin(nq\phi - \omega t), & n = 3k-2 \end{cases}$$

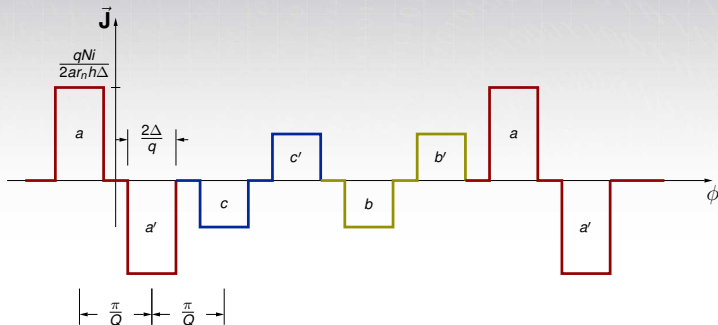
with $k \in \mathbb{N}_1$



Torque Calculation (*cont.*)



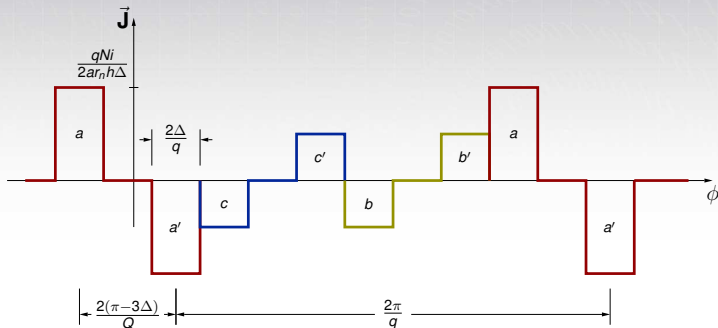
- For the single layer, non-overlapping winding configuration,
 - The $3k-1$ harmonics, 2, 5, 8, ... “moves right”
 - The $3k-2$ harmonics, 1, 4, 7, ... “moves left”



Torque Calculation (*cont.*)



- Similar for the double layer, non-overlapping winding configuration,
 - The $3k-1$ harmonics, 2, 5, 8, ... “moves right”
 - The $3k-2$ harmonics, 1, 4, 7, ... “moves left”



Torque Calculation (*cont.*)



- The netto electromagnetic or mechanical torque, can then be calculated as

$$\begin{aligned}\vec{T}_{mech} &= \int_V \vec{r} \times \vec{f}_v dv \\ &= \int_V r J_z(\phi) B_r^{III}(r, \phi) \vec{a}_z dv\end{aligned}$$

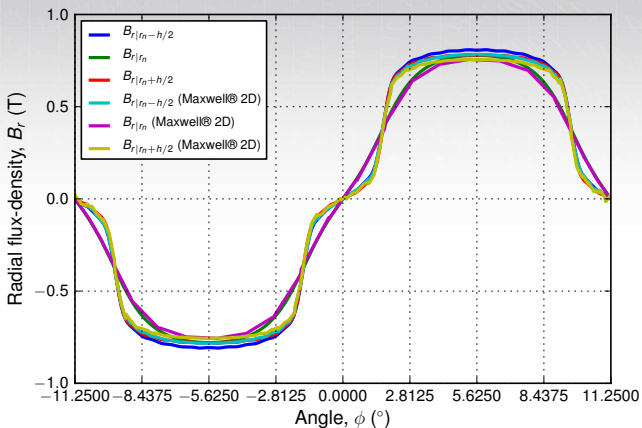
with \vec{r} the radial vector from the centre of the machine, resulting in

$$T_{mech} = \ell \int_{r_n - \frac{h}{2}}^{r_n + \frac{h}{2}} \int_0^{2\pi} r^2 J_z(\phi) B_r^{III}(r, \phi) d\phi dr$$

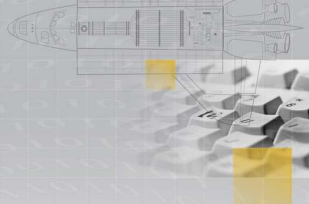
Torque Calculation (cont.)



- Radial flux-density distribution in the centre – as well as on the inner – and outer edge of the stator



Torque Calculation (cont.)



$$T_{mech} = -\frac{3q\ell Nl_p}{ar_n h} \sum_{m=1,5,7,\dots}^{\infty} k_{w,2m} R_m S_m$$

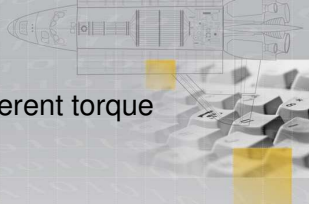
with

$$\begin{aligned} R_m &= \int_{r_n - \frac{h}{2}}^{r_n + \frac{h}{2}} r^2 \cdot \frac{mp(C_m^{III} r^{mp} + D_m^{III} r^{-mp})}{r} dr \\ &= mp \left[\frac{C_m^{III} r^{mp+2}}{mp+2} - \frac{D_m^{III} r^{-mp+2}}{mp-2} \right]_{r_n - \frac{h}{2}}^{r_n + \frac{h}{2}} \end{aligned}$$

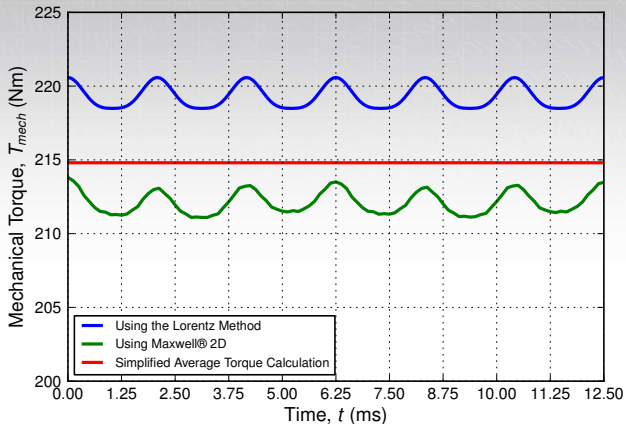
and

$$S_m = \begin{cases} \cos((m-1)p\omega_{mecht}) & \text{for } m=6k+1, k \in \mathbb{N}_0 \\ \sin((m+1)p\omega_{mecht}) & \text{for } m=6k-1, k \in \mathbb{N}_1 \end{cases}$$

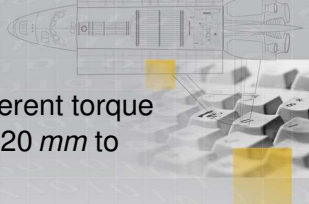
Torque Calculation (*cont.*)



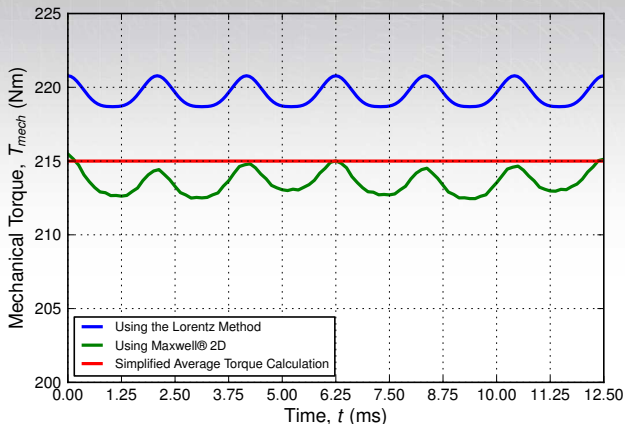
- A comparison between the different torque calculation methods



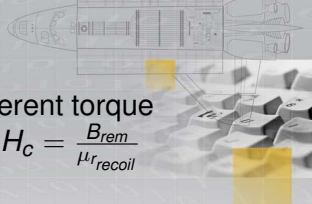
Torque Calculation (*cont.*)



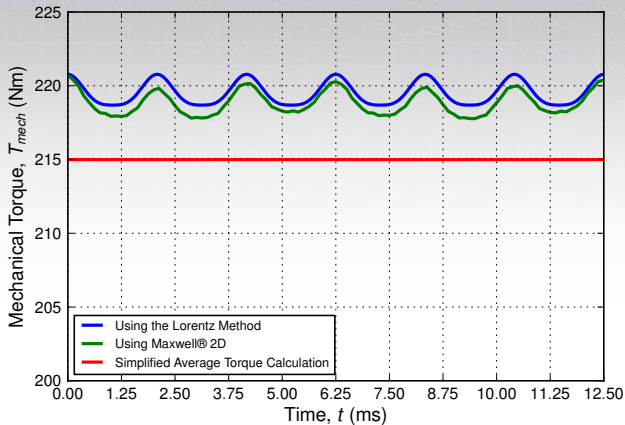
- A comparison between the different torque calculation methods with $h_y = 20 \text{ mm}$ to eliminate rotor yoke saturation



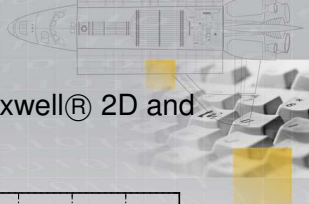
Torque Calculation (*cont.*)



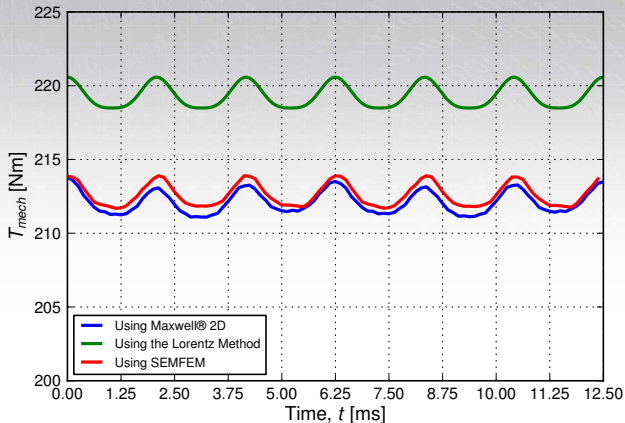
- A comparison between the different torque calculation methods, also with $H_c = \frac{B_{rem}}{\mu_{r_{recoil}}}$



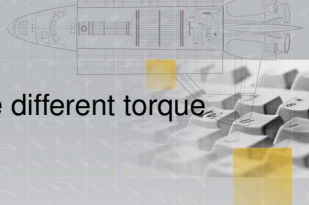
Torque Calculation (*cont.*)



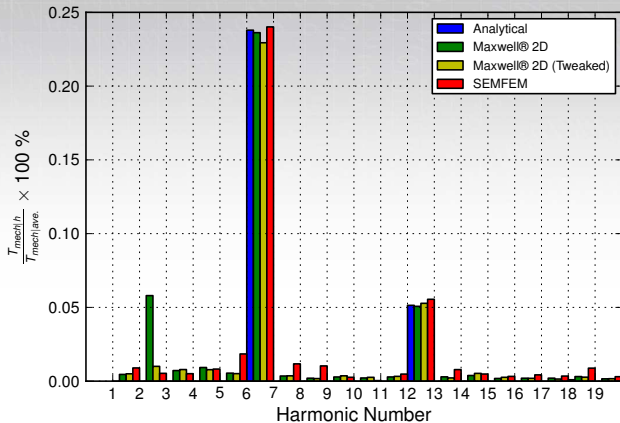
- A comparison between the Maxwell® 2D and SEMFEM, [Gerber et al, 2010]



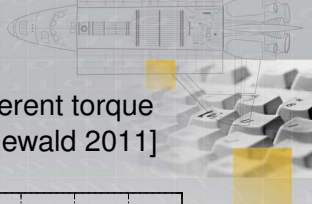
Torque Calculation (*cont.*)



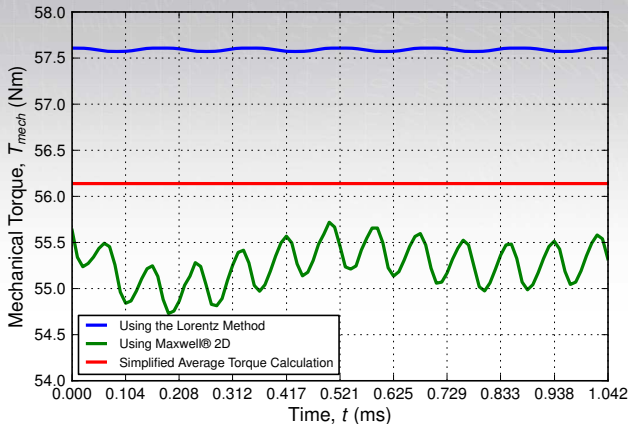
- The harmonic spectrum for the different torque calculation methods:



Torque Calculation (*cont.*)



- A comparison between the different torque calculation methods for [Groenewald 2011]

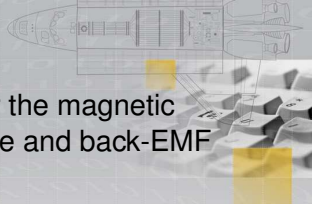


To Conclude

- Sub-domain analysis method provides quick and fairly accurate results for the electromagnetic fields inside a RFAPM machine
- The calculated value of the radial flux density is 3% higher than that using FEM
 - due to the fact that the recoil permeability of the PMs used is not unity and
 - and to a lesser extent, due to the saturation of the iron core yokes
- The analytical solution provided a practical way in which to optimise the pole arc-width of the PMs that would produce a quasi sinusoidal radial flux-density distribution in the centre of the stator windings

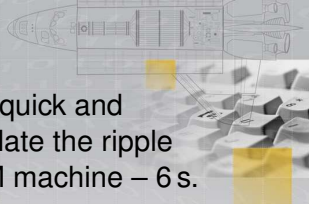
To Conclude (*cont.*)

- From the analytical solution for the magnetic vector potential, the flux-linkage and back-EMF could be calculated
- It was shown that with sinusoidal radial flux-density distribution in the centre of the stator windings a voltage constant, k_E , for the RFAPM machine could be defined, similar to a “normal” brushless DC machine
- From the voltage constant and with the phase current regulated to be in phase with the back-EMF of the RFAPM, a torque constant, $k_T = k_E$, could also be defined

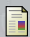


To Conclude (*cont.*)


- the Lorenz method provides a quick and accurate way in which to calculate the ripple torque component of a RFAPM machine – 6 s. vs. ≈ 15 min.
- The 3,3 % error in the torque calculation, compared to FEM, could largely be contributed to the difference in the radial flux-density



Bibliography

- 

M.J. Kamper, R-J. Wang and F.G. Rossouw,
 Analysis and Performance of Axial Flux
 Permanent-Magnet Machine With Air-Cored
 Non-overlapping Concentrated Stator Windings,
IEEE Transactions on Industry Applications,
 May. 2008, p 1495-1504

- 

P.J. Randewijk, M.J. Kamper and R-J. Wang,
 Analysis and Performance Evaluation of Radial
 Flux Air-Cored Permanent Magnet Machines with
 Concentrated Coils,
*Power Electronics and Drives Systems
 Conference, PEDS 2007*

Bibliography (cont.)



J.A. Stegmann


Design and Analysis Aspects of Radial Flux
 Air-cored Permanent Magnet Wind Generator
 System for Direct Battery Charging Applications
Masters Thesis, Stellenbosch University 2010




J.A. Stegmann and M.J. Kamper

Design aspects of medium power double rotor
 radial flux air-cored PM wind generators
*Energy Conversion Congress and Exposition,
 ECCE 2009*

Bibliography (cont.)

- 

J.A. Stegmann and M.J. Kamper
 Design Aspects of Double-Sided Rotor Radial Flux Air-Cored Permanent-Magnet Wind Generator,
IEEE Transactions on Industry Applications,
 Feb. 2011, p 767–778

- 

S. Gerber, J.M. Strauss and P.J. Randewijk
 Evaluation of a hybrid finite element analysis package featuring dual air-gap elements,
Electrical Machines, International Conference on, ICEM-2010

Bibliography (cont.)



D. Groenewald

Evaluation of a radial flux air-cored permanent magnet machine drive with manual transmission drivetrain for electric vehicles,

Masters Thesis, Stellenbosch University 2011